An Epstein-Barr virus–encoded microRNA targets PUMA to promote host cell survival

Elizabeth Yee-Wai Choy,[1] Kam-Leung Siu,[1] Kin-Hang Kok,[1] Raymond Wai-Ming Lung,[4] Chi Man Tsang,[2] Ka-Fai To,[4] Dora Lai-Wan Kwong,[3] Sai Wah Tsao,[2] and Dong-Yan Jin[1]

[1]Department of Biochemistry, [2]Department of Anatomy, and [3]Department of Clinical Oncology, The University of Hong Kong, Pokfulam, Hong Kong
[4]Department of Anatomical and Cellular Pathology, State Key Laboratory in Oncology in South China, Li Ka Shing Institute of Health Science, Prince of Wales Hospital, Chinese University of Hong Kong, Shatin, New Territories, Hong Kong

Epstein-Barr virus (EBV) is a herpesvirus associated with nasopharyngeal carcinoma (NPC), gastric carcinoma (GC), and other malignancies. EBV is the first human virus found to express microRNAs (miRNAs), the functions of which remain largely unknown. We report on the regulation of a cellular protein named p53 up-regulated modulator of apoptosis (PUMA) by an EBV miRNA known as miR-BART5, which is abundantly expressed in NPC and EBV-GC cells. Modulation of PUMA expression by miR-BART5 and anti–miR-BART5 oligonucleotide was demonstrated in EBV-positive cells. In addition, PUMA was found to be significantly underexpressed in ~60% of human NPC tissues. Although expression of miR-BART5 rendered NPC and EBV-GC cells less sensitive to proapoptotic agents, apoptosis can be triggered by depleting miR-BART5 or inducing the expression of PUMA. Collectively, our findings suggest that EBV encodes an miRNA to facilitate the establishment of latent infection by promoting host cell survival.

CORRESPONDENCE
Dong-Yan Jin:
dyjin@hkucc.hku.hk

Abbreviations used: EBER, EBV-encoded small RNA; EBV, Epstein-Barr virus; GC, gastric carcinoma; miRNA, microRNA; NPC, nasopharyngeal carcinoma; PARP, poly (ADP-ribose) polymerase; PUMA, p53 up-regulated modulator of apoptosis; siPUMA, small interfering RNA against PUMA; TUNEL, terminal deoxynucleotidyl transferase–mediated dUTP-biotin nick end labeling; UTR, untranslated region.

Epstein-Barr virus (EBV) is the first human virus shown to be etiologically associated with cancer. Although EBV establishes a lifelong latent infection in >90% of the world's population without serious sequelae, a small fraction of latently infected individuals will develop malignancies of lymphocytic and epithelial origin, such as Burkitt's lymphoma, Hodgkin's lymphoma, extranodal nasal natural killer/T cell lymphoma, nasopharyngeal carcinoma (NPC), and gastric cancer (1, 2). Among nearly 100 viral genes expressed during productive replication, only 11 are expressed in latently infected cells. In addition, EBV was recently found to encode >20 microRNAs (miRNAs) (3–5).

miRNAs are gene regulatory RNAs of ~22 nt in length, and they negatively regulate gene expression either by inducing mRNA degradation or, more commonly in mammalian cells, by repressing translation (6). Cellular miRNAs are critically involved in various biological processes such as development, apoptosis, and proliferation (6). EBV was the first human virus found to encode miRNAs (3). The EBV miRNAs are organized in two clusters within the EBV genome: one in the intronic regions of the BART gene (miR-BART1 to miR-BART-20) and the other in the untranslated regions (UTRs) of the BHRF1 gene (miR-BHRF1-1 to miR-BHRF1-3) (3–5). Conservation of nine EBV miRNAs with counterparts in the rhesus lymphocryptovirus points to the biological importance of these viral miRNAs (4). Interestingly, miR-BARTs were found to be expressed abundantly in latently infected epithelial cells but at a significantly lower level in B cells (4), implicating a role in epithelial carcinogenesis. In further support of this, miR-BARTs were also found to be highly expressed in EBV-associated gastric carcinoma (EBV-GC) cell lines and tissues (7), in which only a few viral genes are constitutively expressed.

The function of most EBV miRNAs is poorly understood. Because miR-BART2 transcript is antisense to that of BALF5 and thus perfectly complementary to its 3′ UTR, miR-BART2 could target BALF5 mRNA for degradation, thereby silencing the expression of

The online version of this article contains supplemental material.

The Rockefeller University Press $30.00
J. Exp. Med. Vol. 205 No. 11 2551-2560
www.jem.org/cgi/doi/10.1084/jem.20072581

BALF5 viral DNA polymerase to inhibit lytic replication (3, 8). Another recent study implicated the involvement of miR-BHRF1-2 in the cleavage of BHRF1 RNA in the cytoplasm (9). In contrast, an inverse correlation between expression levels of miR-BHRF1-3 and CXCL-11, which is an interferon-inducible T cell–attracting chemokine, implicated an immunomodulatory function of the viral miRNA in lymphomas (10). In addition, miR-BARTs were also found to regulate the expression of LMP1 viral oncoprotein (11). Although EBV miRNAs are important regulators of viral gene expression, they may also target cellular transcripts to facilitate viral persistence and oncogenesis. Indeed, potential cellular targets of EBV miRNAs predicted by in silico analysis include growth regulators, modulators of apoptosis, B cell–specific chemokines and cytokines, transcriptional regulators, and signal transducers (3). However, experimental evidence for the control of cellular gene expression by EBV miRNAs remains to be established.

In this study, we sought to shed light on the roles of miR-BARTs in establishing latent infection and driving carcinogenesis in epithelial cells through identification and characterization of their cellular targets. By bioinformatic analysis and functional screening, p53 up-regulated modulator of apoptosis (PUMA), also known as BBC3 (Bcl2 binding component 3), was found to be targeted by miR-BART5. PUMA is a pro-apoptotic protein belonging to the "BH3-only" group of the Bcl-2 family (12–14). Although it is an immediate downstream target of p53, PUMA can also induce p53-independent apoptosis in response to a wide variety of stimuli (12, 15–17). In this paper, we provide the first evidence for the suppression of PUMA expression by miR-BART5. Overexpression and loss-of-function experiments were performed to characterize the function of miR-BART5. The expression of PUMA in human NPC tissues was also examined. In addition, the functional implications of miR-BART5–mediated silencing of PUMA in the survival of EBV$^+$ NPC and GC cells were investigated. Our work reveals a new molecular mechanism through which EBV confers resistance to apoptosis in NPC cells by counteracting the proapoptotic function of p53/PUMA with a viral miRNA.

RESULTS

Identification of PUMA as a cellular target of miR-BART5

We predicted cellular targets of all miR-BARTs using miRanda (18, 19) and RNAhybrid (20) programs, which have previously been shown to be successful in target prediction (21). The top candidates for each miR-BART (for a list of top candidates for miR-BART5 see Table S1, available at http://www.jem.org/cgi/content/full/jem.20072581/DC1) were validated with reporter assays. Synthetic target sites were inserted into 3′ UTR of luciferase gene, and the influence of miR-BART on luciferase expression was assessed. miR-BART5 was chosen for further study because the most pronounced gene-silencing effect on a cellular target named PUMA was observed with this miRNA in the reporter assay. Actually, out of nine potential cellular targets shortlisted, PUMA was the only one that was shown to be suppressed by miR-BART5 in the reporter assay (Table S1).

The predicted miR-BART5 target site in the 3′ UTR of PUMA exhibited good complementarity to miR-BART5 and was highly conserved among human, chimp, rhesus monkey, and mouse (Fig. 1 A). Although a 7-nt stretch that perfectly matches the 5′ seed region of miR-BART5 was found in the predicted site, there were multiple mismatches in the central region (Fig. 1 A, top).

Although there are four isoforms of PUMA (α, β, γ, and δ), all isoforms conserve the same 3′ UTR and only two isoforms (PUMA-α and PUMA-β) have proapoptotic activity (13). To validate the interaction of miR-BART5 with the 3′

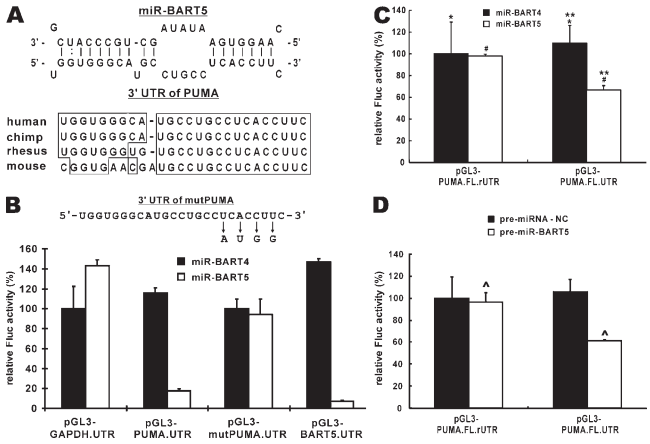

Figure 1. PUMA is a cellular target of miR-BART5. (A) Target site of miR-BART5 in 3′ UTR of PUMA. The top shows the sequences in the 3′ UTR of PUMA that base pair with miR-BART5. The bottom shows the conservation of the target site sequences in different species of vertebrates. Conservative nucleotides are boxed. (B) Functional characterization of miR-BART5 target site. pGL3-PUMA.UTR has target sites of miR-BART5 inserted into the 3′ UTR of luciferase gene. This reporter construct was cotransfected into HeLa cells with an expression vector for either miR-BART4 or miR-BART5. Plasmids pGL3-BART5.UTR and pGL3-GAPDH served as positive and negative controls, respectively. These control plasmids are different from pGL3-PUMA.UTR only in the 3′ UTR of luciferase gene. pGL3-BART5.UTR contains target sequences perfectly matched with miR-BART5, whereas pGL3-GAPDH.UTR harbors irrelevant GAPDH sequences. In pGL3-mutPUMA.UTR, the target sites of miR-BART5 in the PUMA 3′ UTR were mutated as indicated in the top. The relative luciferase activity was obtained by normalizing the readings of the firefly luciferase (Fluc) activity from the pGL3 vector with those of the *Renilla reniformis* luciferase activity from pRL-CMV. Results represent mean ± SD from three independent experiments. (C and D) Functionality of miR-BART5 target site in PUMA 3′ UTR. A single copy of the entire PUMA 3′ UTR sequence was inserted into the 3′ UTR of luciferase gene to generate pGL3-PUMA.FL.UTR. This reporter construct was cotransfected into HeLa cells with an expression vector for either miR-BART4 or miR-BART5, or with commercially available synthetic RNA oligonucleotides pre-miRNA-NC or pre-miR-BART5. Plasmid pGL3-PUMA.FL.rUTR, in which a reversed single copy of the PUMA 3′ UTR sequence was inserted into the 3′ UTR of luciferase gene, served as a negative control. Error bars indicate SD (n = 3). *, P = 0.2819 (by Student's t test); **, P = 0.0346; #, P = 0.0042. ^, P = 0.0069.

UTR of PUMA, luciferase reporter assays were performed. Four copies of a PUMA 3′ UTR fragment containing the predicted miR-BART5 target site were cloned into the 3′ UTR of the firefly luciferase gene. The resulting plasmid termed pGL3-PUMA.UTR was cotransfected into HeLa cells with the miR-BART5 expression vector, in which the expression of miR-BART5 was driven by the strong H1 promoter (22). Significant reduction of luciferase activity induced by miR-BART5 indicated that the miR-BART5 target site in PUMA 3′ UTR is functional (Fig. 1 B). The specificity of miR-BART5–mediated silencing of PUMA was further supported by several controls in the experiment. First, miR-BART4, another miRNA encoded by EBV, did not show any inhibitory effect on PUMA 3′ UTR–dependent expression of luciferase gene. Second, miR-BART5 did not inhibit luciferase gene expression under the control of GAPDH sequences in cells receiving the pGL3-GAPDH.UTR reporter construct. Third, miR-BART5 suppressed reporter gene expression to similar magnitudes in cells receiving the pGL3-PUMA.UTR plasmid and the pGL3-BART5.UTR vector having 3′ UTR sequences perfectly complementary to miR-BART5. Finally, when the miR-BART5 target sequences in PUMA 3′ UTR were point mutated to disrupt complementarity to the seed region of miR-BART5 (Fig. 1 B, top), the inhibition of luciferase expression by miR-BART5 was completely abolished.

A criticism of this experiment is that multiple copies of partial 3′ UTR sequence of PUMA were used. To address this issue, we constructed a plasmid in which a single copy of the entire 3′ UTR of PUMA controls the expression of luciferase reporter. When we repeated the reporter assay with this construct, luciferase activity was significantly decreased in cells expressing miR-BART5 (Fig. 1 C). This effect was specific, as no such inhibition was observed when miR-BART4 was expressed. Likewise, specific suppression of luciferase activity under the control of a single copy of the entire 3′ UTR of PUMA was only seen in cells transfected with pre–miR-BART5, a chemically synthesized precursor miRNA (Fig. 1 D). All these results consistently indicated specific targeting of PUMA 3′ UTR by miR-BART5.

Expression of miR-BART5 in EBV-infected epithelial cells

For miR-BART5 to fulfill a gene regulatory function, it has to be expressed in EBV-infected cells. Because miR-BARTs were thought to be expressed preferentially in EBV-infected epithelial cells (4, 7), we tested miR-BART5 expression in C666-1, an NPC cell line that constitutively harbors EBV (23). For comparison, we also examined HK1, another NPC cell line that does not carry EBV (24). In addition, the HK1/EBV cell line, to which EBV was reintroduced by coculture with infected Akata cells (25), was also included. Consistent with previous reports (4, 11), ample amount of miR-BART5 was found in C666-1 cells (Fig. 2 A, lane 3). The expression level of miR-BART5 in C666-1 cells was comparable to that in HEK293 cells stably transfected with miR-BART5 expression vector (Fig. 2 A, lane 5). As a control, miR-BART3-5p, another miRNA encoded by EBV, was also detected in C666-1 cells. Although no miR-BART5 was found in HK1 cells, the expression signal of miR-BART5 in HK1/EBV was visible after longer exposure of the blot (Fig. 2 A, lanes 1 and 2).

Because miR-BARTs were also shown to be abundant in EBV-GC cells (7), the expression of miR-BART5 in AGS/BX1 was examined. AGS/BX1 cell line was established through infection of AGS cells with recombinant EBV virus carrying a GFP gene (26). We noted that miR-BART5 was expressed in AGS/BX1 but not in EBV-negative AGS cells (Fig. 2 A, lane 7 compared with lane 6). In contrast, miR-BART5 was not expressed in B95-8 cells (Fig. 2 B, lane 9; and Fig. S1, lane 21, available at http://www.jem.org/cgi/content/full/jem.20072581/DC1) carrying a laboratory strain of EBV with a deletion in the miR-BART5 region (4). In addition, miR-BART5 was hardly found in other EBV-infected Burkitt's lymphoma cell lines, Akata, Namalwa, and Raji (Fig. S1, lanes 18–20). Thus, miR-BART5 was preferentially expressed in EBV-infected NPC and GC cells.

We next extended our analysis of miR-BART5 expression to primary NPC tumor tissues and xenografts that had been verified to be positive for EBV-encoded small RNA (EBER). miR-BART5 was abundantly expressed in all NPC tumor

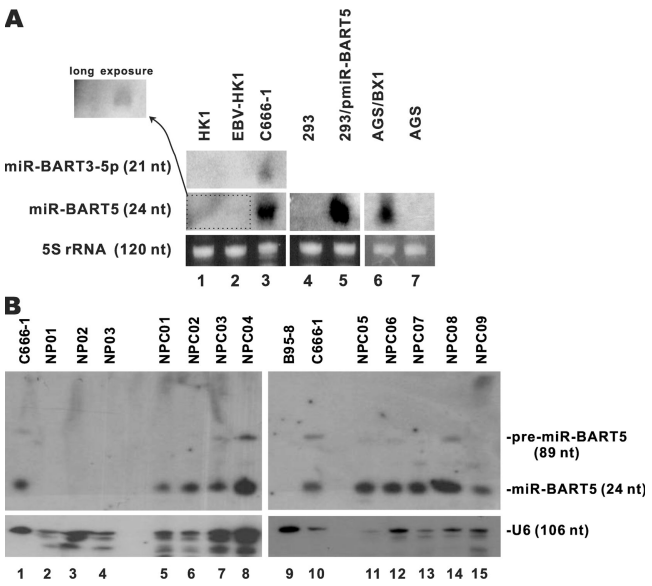

Figure 2. Expression of miR-BART5 in EBV-infected epithelial cells (A) Northern blot analysis of EBV miRNAs in NPC and EBV-GC cell lines. HK1, HK1/EBV, and C666-1 are NPC cell lines (lanes 1–3). AGS/BX1 is an EBV-GC cell line (lane 6). Untransfected HEK293 cells (293; lane 4), HEK293 cells stably expressing miR-BART5 (293/pmiR-BART5; lane 5), and AGS cells (lane 7) were included as controls. Expression signal of miR-BART5 in HK1/EBV cells was visible only after long exposure (inset). The 5S rRNA served as a loading control. Although lanes 1–5 in the middle were from the same exposure of one experiment, lanes 6 and 7 were from another experiment. (B) Northern blot analysis of miR-BART5 in human NPC tissue samples. Three normal nasopharyngeal biopsies (NP01, NP02, and NP03; lanes 2–4) and nine NPC tumor samples (NPC01 to NPC09; lanes 5–8 and 11–15) were analyzed. C666-1 and latency III B95-8 lymphoblastoid cells (lanes 1, 9, and 10) were included as positive and negative controls, respectively. U6 small nuclear RNA served as a loading control.

samples to a level comparable with or even higher than that in C666-1 cells (Fig. 2 B, lanes 5–8 and 11–15; and Fig. S1, lanes 10, 16, and 17). In addition, most of the xenografts originally derived from NPC tumor were also strongly positive for miR-BART5 (Fig. S1, lanes 4, 5, 7, 14, and 15). In sharp contrast, miR-BART was not found in normal nasopharyngeal tissues obtained from three different subjects (Fig. 2 B, lanes 2–4). Hence, miR-BART5 was abundantly expressed in EBV-infected NPC tumor samples. This is consistent with reported expression pattern of miR-BART miRNAs in NPC and non-NPC samples (4, 11).

PUMA expression in NPC cells and tissues

As demonstrated in the previous section, abundant miR-BART5 expression was observed in EBV-infected epithelial cells and tissues. If miR-BART5 functions to counteract PUMA, a significant decrease of PUMA expression should occur in EBV$^+$ NPC cells expressing miR-BART5. To address this issue, we compared the expression levels of PUMA in HK1 and HK1/EBV cells. These two NPC cell lines were chosen because HK1/EBV was derived from HK1 and it represents the EBV$^+$ counterpart of HK1 (24, 25). The expression of PUMA-α and PUMA-β in HK1/EBV cells was diminished 2–2.5-fold when compared with the level in HK1 cells (Fig. 3 A). Consistent with this, specific and statistically significant ($P < 0.0027$ by Student's *t* test) inhibition of luciferase expression from plasmid pGL3-PUMA.UTR was observed in HK1/EBV cells but not in HK1 cells (Fig. S2, available at http://www.jem.org/cgi/content/full/jem.20072581/DC1). These results are in accordance with viral modulation of PUMA expression plausibly through miR-BART5.

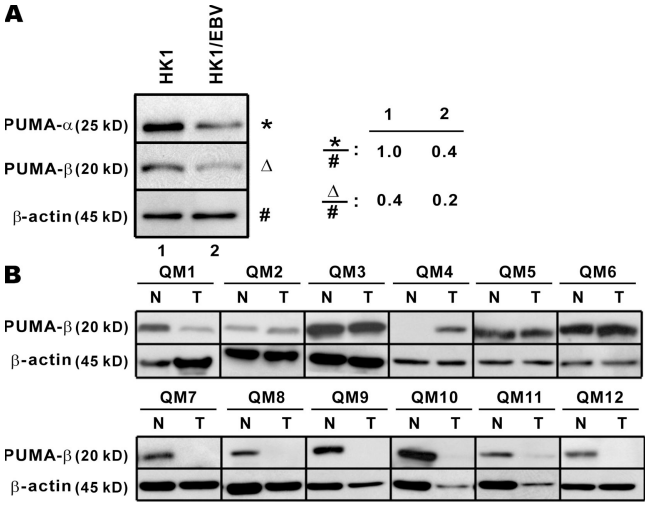

Figure 3. Endogenous PUMA protein expression in EBV$^+$ NPC cell line and human primary NPC tissue samples. (A) Western blot analysis of PUMA-α and PUMA-β proteins in miR-BART5–expressing HK1/EBV cells versus EBV$^-$ HK1 cells. (B) Western blot analysis of PUMA-β protein expression in 12 pairs of primary NPC tissue samples and noncancerous nasopharyngeal tissue samples. N, noncancerous nasopharyngeal tissue; T, tumorous NPC tissue.

To verify the expression state of PUMA in human NPC, we determined the amounts of PUMA-β protein in 25 pairs of matched NPC and non-NPC samples. The NPC and non-NPC samples were collected from the same patient diagnosed with undifferentiated carcinoma, which is the most common histology in this region and associated with EBV (2). Consistent with results shown in Fig. 2 B and with a previous study (27), expression of viral markers EBER and BART in all NPC samples, as well as the absence of these markers in all non-NPC samples, were verified by RT-PCR (not depicted). Because of limited amount of sample, Northern blot analysis of miR-BART5 expression in the same sample was not possible. Among the 25 pairs of samples, a drop of PUMA-β protein expression was detected in ∼60% of the NPC tissues compared with their corresponding non-NPC tissues. Notably, PUMA-β expression was undetectable in many NPC samples. For example, in 12 representative pairs of NPC and non-NPC samples randomly selected (Fig. 3 B), PUMA-β was diminished in 7 NPC samples (samples QM1, QM7, QM8, QM9, QM10, QM11, and QM12), among which a complete loss of PUMA expression was seen in 5 samples (samples QM7, QM8, QM9, QM10, and QM12). Considered together with results shown in Fig. 1 and Fig. 2, we inferred that the expression of miR-BART5 was associated with severe inhibition of PUMA in undifferentiated NPC tissues.

Modulation of endogenous PUMA expression by miR-BART5

The above results provided the first experimental evidence for the regulation of PUMA expression by miR-BART5 of EBV. To test this idea more directly, we introduced pre–miR-BART5, the specificity of which had been verified in Fig. 1 D, into PUMA-expressing HeLa cells. When the miR-BART5 precursor RNA was expressed in the cells, substantial reduction in PUMA-β protein expression was observed, but this reduction was not seen in cells transfected with negative control precursor RNA (pre–miRNA-NC; Fig. 4 A, lanes 1 and 2). Likewise, a decline in PUMA-β expression was also observed when pre–miR-BART5 was overexpressed in HK1 cells (Fig. 4 A, lane 4 compared with lane 3). Because of difference in transfection efficiency (unpublished data), the magnitude of PUMA protein reduction in HK1 cells was not as great as in HeLa cells. To investigate the influence of miR-BART5 on the expression of PUMA mRNA, RT-PCR was performed with cells transfected with miR-BART5 expression vector. Although PUMA transcript was amply found in cells that expressed miR-BART3-5p, it was undetectable in miR-BART5-expressing cells (Fig. 4 B). Hence, regulation of PUMA protein expression by miR-BART5 was associated with decreased level of PUMA mRNA. This is consistent with the model in which mRNAs translationally repressed by miRNAs might be stored in the P-bodies and subsequently degraded (28, 29).

Enforced expression of miR-BART5 in HeLa and HK1 cells led to inhibition of PUMA expression (Fig. 4, A and B). In contrast, miR-BART5 was abundantly expressed in C666-1 and AGS/BX1 cells (Fig. 2 A). If miR-BART5 is an inhibitor

of PUMA expression, it should prevent the accumulation of PUMA protein in both C666-1 and AGS/BX1 cells. In other words, compromising the function of endogenous miR-BART5 in C666-1 cells should induce derepression of PUMA expression. Indeed, elevation of PUMA-α and PUMA-β proteins was observed in C666-1 cells when miR-BART5 was specifically inhibited with an anti–miR-BART5 oligonucleotide (Fig. 4 C). Consistent with this, luciferase reporter assay driven by PUMA 3′ UTR was also found to be increased in C666-1 cells transfected with anti–miR-BART5 (Fig. S3, available at http://www.jem.org/cgi/content/full/jem.20072581/DC1). Likewise, an increase in the steady-state amount of PUMA-β protein was detected in AGS/BX1 cells transfected with anti–miR-BART5 (Fig. 4 D). These results corroborated the notion that the expression of PUMA was effectively repressed by miR-BART5 in EBV$^+$ epithelial cells.

miR-BART5 protects host cells from apoptosis

In the previous section, we presented several lines of evidence to support the regulation of PUMA by miR-BART5 in NPC cells. The importance of PUMA in mediating apoptosis prompted us to explore whether miR-BART5 inhibition of PUMA in NPC cells confers resistance to apoptosis. We compared the sensitivity of C666-1 and NP69 cells to adriamycin, a DNA-damaging agent that induces apoptosis. NP69 is an EBV$^-$ nasopharyngeal epithelial cell line, which is commonly used as a non-NPC counterpart of C666-1 (23, 30, 31). In line with our finding on the underexpression of PUMA in HK1/EBV cells (Fig. 3 A), the basal level of PUMA-β protein in C666-1 cells was significantly lower than in NP69 cells (Fig. 5 A). In addition, treatment with adriamycin induced PUMA-β expression in NP69 cells, but no significant induction was seen in C666-1 cells. Consistent with this, a majority of poly (ADP-ribose) polymerase (PARP) protein was found to be cleaved in NP69 cells treated with 0.8 μg/ml or 1.2 μg/ml adriamycin, but the percentages of cleaved PARP were much smaller in C666-1 cells treated with the same concentrations of adriamycin (Fig. 5 A). The cleavage of PARP by caspase 3 facilitates cellular disassembly and serves as a sensitive marker of apoptosis (32). Thus, our results suggested that C666-1 cells expressing less PUMA-β were more resistant to apoptosis. A similar observation was also made with AGS/BX1 and HK1/EBV cells, which were less prone

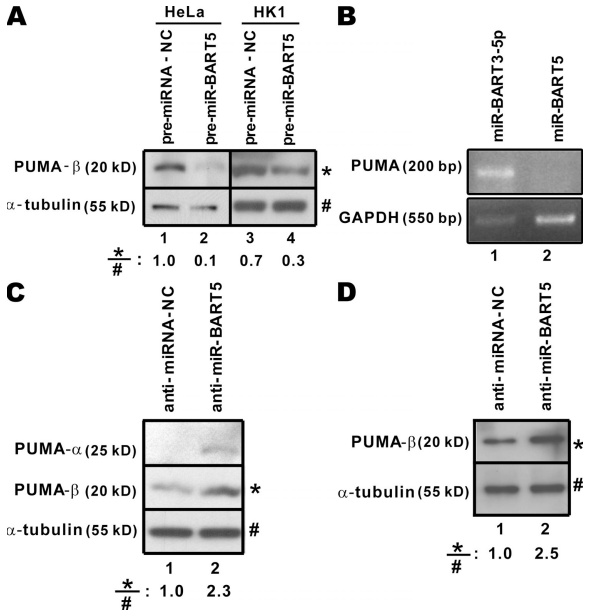

Figure 4. Modulation of PUMA expression by miR-BART5. (A) Down-regulation of PUMA-β protein expression by pre–miR-BART5. Pre–miR-BART5 and pre–miRNA-NC were introduced into HeLa and HK1 cells. Expression of PUMA-β and α-tubulin proteins was analyzed by Western blotting. Relative PUMA-β protein amounts are shown at the bottom. (B) Down-regulation of PUMA mRNA expression by miR-BART5. miR-BART3-5p or miR-BART5 expression vector was transfected into HEK293 cells. PUMA and GAPDH transcripts were analyzed by RT-PCR. (C and D) Up-regulation of PUMA expression by anti–miR-BART5 in C666-1 and AGS/BX1 cells. Anti–miR-BART5 oligonucleotide inhibitor was transfected into miR-BART5–expressing C666-1 cells. Endogenous PUMA-α and PUMA-β proteins were detected by Western blotting. An irrelevant anti-miRNA oligonucleotide (anti–miRNA-NC) was used as a negative control. Relative PUMA-β protein amounts are shown at the bottom.

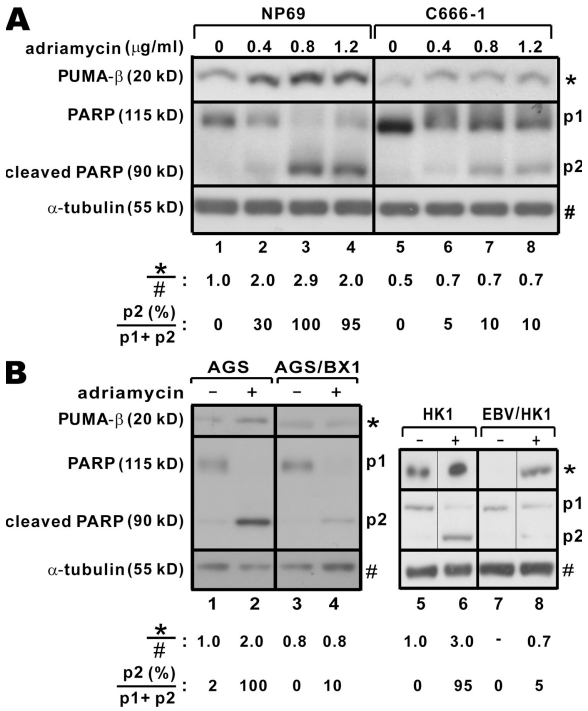

Figure 5. EBV confers resistance to apoptosis. (A) Sensitivity of NP69 and C666-1 cells to adriamycin. EBV$^-$ NP69 and EBV$^+$ C666-1 cells were treated with indicated concentrations of adriamycin for 48 h. PUMA-β, PARP and α-tubulin proteins were analyzed by Western blotting. Shown at the bottom are relative expression levels of PUMA-β and percentages of cleaved PARP. (B) Sensitivity of AGS, AGS/BX1, HK1, and HK1/EBV cells to adriamycin. Cells were treated with 1.5 μg/ml (AGS and AGS/BX1 cells) or 1.2 μg/ml (HK1 and EBV/HK1) adriamycin for 48 h. Black lines indicate that intervening lanes have been spliced out.

to apoptosis than their respective parental cells (Fig. 5 B, lane 4 compared with lane 2 and lane 8 compared with lane 6). Thus, miR-BART5–expressing cells (C666-1, AGS/BX1 and HK1/EBV) are less susceptible to apoptosis-inducing drugs.

Interestingly, we found that the resistance to apoptosis occurred only in C666-1 cells treated with low-dose adriamycin (<1.2 μg/ml). Apoptosis was induced when the concentration of adriamycin was increased to 1.5 μg/ml or higher. Likewise, C666-1 cells treated with 80 μM etoposide also underwent apoptosis (Fig. 6). The manifestation of apoptosis in treated C666-1 cells was indicated by PARP cleavage (Fig. 6 A) and by terminal deoxynucleotidyl transferase–mediated dUTP-biotin nick end labeling (TUNEL) assay, which measures DNA fragmentation (Fig. 6 B and Fig. S4, available at http://www.jem.org/cgi/content/full/jem.20072581/DC1). To investigate the underlying mechanism of apoptosis, we determined the expression profile of p53 and PUMA-β. Interestingly, both p53 and PUMA-β were induced significantly by high-dose adriamycin and etoposide (Fig. 6 A). Collectively, our results are compatible with the notion that the steady-state amount of PUMA dictates cellular sensitivity to proapoptotic agents. According to this model, when PUMA expression in C666-1 cells was effectively blocked by miR-BART5, apoptosis was prevented (Fig. 5). However, if the inhibitory effect of miR-BART5 was overcome by high-dose proapoptotic agents, apoptosis was triggered (Fig. 6).

To further strengthen this model, we asked whether inhibition of miR-BART5 by another means would also induce apoptosis. Because miR-BART5 can be specifically and effectively inhibited by anti–miR-BART5 oligonucleotide (Fig. 4, C and D), we tested the influence of this miR-BART5 inhibitor on apoptosis of C666-1 and AGS/BX1 cells. Notably, transfection of C666-1 cells with anti–miR-BART5 oligonucleotide triggered apoptosis (Fig. 7 A and Fig. S5, available at http://www.jem.org/cgi/content/full/jem.20072581/DC1). Additionally, anti–miR-BART5 oligonucleotide was able to enhance the proapoptotic effect of etoposide mildly leading to an ~10% increase of TUNEL-positive apoptotic cells (Fig. 7 A). Plausibly, both anti–miR-BART5 oligonucleotide and etoposide exert their proapoptotic effects by inducing the expression of PUMA.

To verify that the effect of anti–miR-BART5 is indeed mediated through PUMA, we made use of small interfering RNA against PUMA (siPUMA), a validated siRNA targeting PUMA transcripts. As a first step, the effectiveness of siPUMA

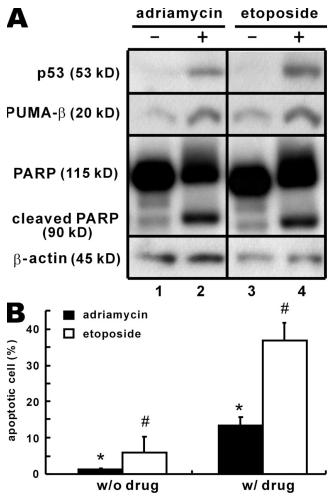

Figure 6. Induction of PUMA expression in C666-1 cells leads to apoptosis. (A) Western blot analysis of PARP. C666-1 cells were treatment with either 1.5 μg/ml adriamycin or 80 μM etoposide for 48 h. Expression of p53, PUMA-β, PARP, and β-actin was examined by Western blotting. (B) TUNEL analysis of apoptotic cells. TUNEL assays were performed on adriamycin- or etoposide-treated C666-1 cells by using confocal microscopy. Representative images are shown in Fig. S4 (available at http://www.jem.org/cgi/content/full/jem.20072581/DC1). 250 cells were scored, and the quantitative results represent mean ± SD from three independent experiments. *, P = 0.035 (by Student's *t* test); #, P = 0.011.

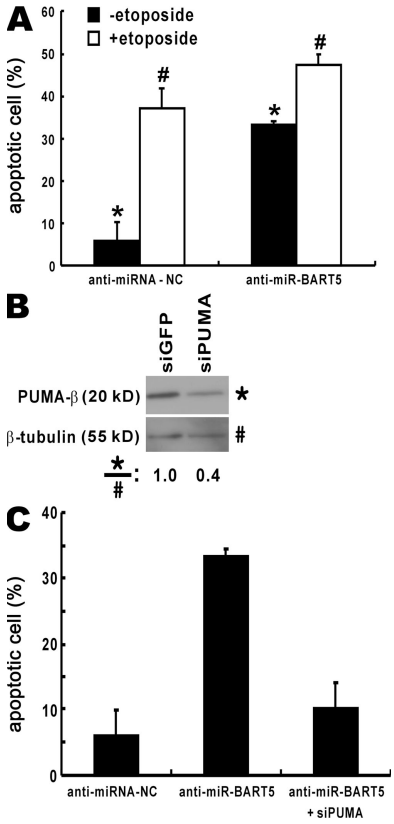

Figure 7. Inhibition of miR-BART5 in C666-1 cells induces apoptosis. (A) Induction of apoptosis. C666-1 cells were transfected with anti–miR-BART5 or anti–miRNA-NC oligonucleotide inhibitor. Cells were treated with etoposide as in Fig. 6 and TUNEL assay was performed. Representative images are shown in Fig. S5 (available at http://www.jem.org/cgi/content/full/jem.20072581/DC1). 250 cells were scored and the quantitative results represent mean ± SD from three independent experiments. *, P = 0.03 (by Student's *t* test); #, P = 0.05. (B) Suppression of PUMA expression by siRNA. C666-1 cells were transfected with 100 nM siGFP or siPUMA. Expression of PUMA-β was examined by Western blotting. (C) Inhibition of miR-BART5 activity by siPUMA. C666-1 cells were co-transfected with anti–miR-BART5 and siPUMA. Apoptotic cells were analyzed as in A. Error bars indicate SD (*n* = 3).

was confirmed by Western blot analysis of PUMA-β (Fig. 7 B). We then cotransfected both anti–miR-BART5 and siPUMA into C666-1 cells and assessed the impact on apoptosis. A partial but significant suppression of anti–miR-BART5–dependent proapoptotic activity by siPUMA (Fig. 7 C) provided further support to our model.

Additionally, transfection of AGS/BX1 cells with anti–miR-BART5 also induced apoptosis, but to a lesser extent (Fig. S6, available at http://www.jem.org/cgi/content/full/jem.20072581/DC1). This weaker effect might be ascribed to a higher basal level of apoptosis in anti–miRNA-NC–transfected AGS/BX1 cells, which had been selected with G418. Collectively, our results consistently demonstrated that miR-BART5 protects host epithelial cells from apoptosis.

DISCUSSION

In this study, we provided the validation of a cellular target of EBV miRNA and characterized the antiapoptotic function of an EBV miRNA. Three lines of evidence were presented to support the regulation of PUMA protein expression by miR-BART5 in EBV-infected epithelial cells. First, an miR-BART5 target site in the 3′ UTR of PUMA transcript was identified and validated (Fig. 1 and Fig. S2). Second, abundant expression of miR-BART5 in NPC cells (Fig. 2 and Fig. S1) correlated with significant underexpression of PUMA in ∼60% of NPC tissues (Fig. 3). Third, manipulation of miR-BART5 expression in NPC cells and an miR-BART5 producing carcinoma cells from another origin (EBV-GC cells) by overexpression and depletion with an oligonucleotide inhibitor resulted in repression and derepression of PUMA expression, respectively (Fig. 4). More importantly, miR-BART5 was shown to have antiapoptotic activity in both NPC and EBV-GC cells. Although EBV^+ NPC and EBV-GC cells were found to be less susceptible to apoptosis (Fig. 5), induced expression of endogenous PUMA by either pharmaceutical agent or anti–miR-BART5 oligonucleotide triggered apoptotic death of these cells (Figs. 5–7 and S3–S5). Our findings suggest a new mechanism for the survival of EBV-infected epithelial cells in which miR-BART5 targets PUMA to confer resistance to apoptosis. This work has important implications not only in EBV biology and pathogenesis, but also in the development of new anti-EBV and anticancer agents.

Herpesviruses encode various miRNAs to regulate viral replication and to counteract host defense such as apoptosis and immunity (33). For example, CMV exploits miR-UL112-1 to evade immune surveillance by suppressing MICB gene (34) and to inhibit expression of the major immediate-early genes (35). In EBV, >20 viral miRNAs are categorized into two main groups, namely miR-BHRF1 and miR-BARTs (3–5). Although some of the EBV miRNAs are thought to modulate viral gene expression by targeting BALF5 and LMP1 (3, 11), miR-BHRF1-3 has been proposed to repress expression of a chemokine named CXCL-11, which attracts T cells in response to interferons (10). It is noteworthy that other viral genes in the BHRF1 and BART regions also have regulatory function in apoptosis and cell signaling. As such, BHRF1 gene encodes an antiapoptotic Bcl-2 homologue that enhances cell survival (36), whereas several protein products derived from BART mRNAs can modulate Notch signaling and RACK1-orchestrated activities (37, 38). miR-BART5 was derived from an intron of BART transcript. Although our findings on miR-BART5 reveal another level of complexity in the functions of BART transcripts during EBV infection, the PUMA-suppressing and antiapoptotic properties of miR-BART5 are generally consistent with existing knowledge on BARTs and EBV miRNAs. Our demonstration of the antiapoptotic function of miR-BART5 from EBV provides the first example for viral modulation of apoptosis through an miRNA. Plausibly, different viral miRNAs might target different cellular proapoptotic proteins to promote host cell survival.

Although PUMA has the ability to mediate p53-independent apoptosis, it remains an immediate and important downstream target of p53 (12–17). p53 and PUMA are master regulators of cellular growth and apoptosis. In view of the recent finding that miR-34s are direct transcriptional targets of p53, the link between p53 and miRNAs is closer than expected (39). However, one missing piece in the p53-miRNA puzzle is the regulation of p53 and p53 targets by miRNAs. In this perspective, our findings on the modulation of PUMA expression by miR-BART5 add a new dimension to our knowledge of p53 and miRNA. It remains to be elucidated whether p53 and PUMA might be targeted by other viral and cellular miRNAs.

Notably, Kaposi's sarcoma–associated herpesvirus miR-K12-11 is an orthologue of cellular miR-155 (40, 41). In addition, miR-BART5 of EBV shares significant seed homology with cellular miR-18a and miR-18b (42). Although cellular miRNAs that target PUMA have not been identified, we cannot rule out the possibility that miR-BART5 and a cellular miRNA might target the same 3′ UTR sequence of PUMA mRNA. Hence, additional experiments are required to clarify whether the anti–miR-BART5 oligonucleotide used in our study might also affect unidentified cellular miRNAs that regulate PUMA expression.

The modulation of PUMA by miR-BART5 was not surprising. In NPC, p53 is rarely mutated (43) but commonly activated likely through LMP1 (44). Thus, EBV has to develop counter measures against p53 activation of PUMA to persist within the host cell. As demonstrated in our study, EBV can express ample amount of miR-BART5 to down-regulate the expression of proapoptotic PUMA in NPC and GC cells latently infected by EBV. This might explain the particularly high expression of miR-BART5 in epithelial cancer cells when compared with EBV-positive lymphoma cells. It is also noteworthy that the underexpression of PUMA was observed only in ∼60% of the $BART^+$ NPC tissue samples (Fig. 3). This raises the possibility that PUMA expression might be governed by more than one mechanism during EBV infection and carcinogenesis.

Our work has derived one new mechanism for EBV modulation of apoptosis. Based on this mechanism, new strategies can be devised to develop diagnostic tools and therapeutic agents. For example, the detection of miR-BART5

could be useful in the diagnosis of NPC and EBV-GC. In addition, miR-BART5 is a potential therapeutic target in NPC, EBV-GC, and other EBV-associated epithelial malignancies. The use of anti–miR-BART5 oligonucleotide inhibitor to specifically induce apoptosis in epithelial cancer cells may prove useful in anti-EBV and anti-cancer therapy.

MATERIALS AND METHODS

Target prediction. miRanda (18) and RNAhybrid (20) were used to predict the potential targets of EBV miRNAs. Human 3′ UTR sequences were retrieved using BioMart (http://www.ensembl.org/Multi/martview) and subsequently fed into miRanda for prediction, with an energy threshold of −20 kcal/mol and a cutoff score of 120 to increase the stringency. Potential targets ranked within the top 50 (see Table S1 for a list of potential targets of miR-BART5 predicted by miRanda) were then reanalyzed using RNAhybrid. Cross species conservation was also assessed using University of California Santa Cruz Human BLAT (http://genome.ucsc.edu/cgi-bin/hgBlat?command=start). Potential target sites with a minimum free energy of <−30 kcal/mol, as predicted by RNAhybrid, were shortlisted for functional screening with luciferase reporter assays.

For prediction of miR-BART5 targets, nine potential targets were obtained after analysis by miRanda and RNAhybrid. Although PUMA was ranked 43rd in the list of targets predicted by miRanda, it was selected for validation by reporter assay because the target site was predicted to have a minimum free energy of −30.7 kcal/mol (Table S1). Among all potential target sites verified by reporter assay, PUMA was the only one that was suppressed by miR-BART5 (Table S1).

Cell culture, transfection, and reporter assay. HeLa and HEK293 cell lines; human NPC cell lines C666-1, HK1, and HK1/EBV; human EBV-GC cell line AGS/BX1 and its parental line AGS (provided by H. Chen and B. Wong, University of Hong Kong, Pokfulam, Hong Kong); human nasopharyngeal cell lines NP69 and NP460; and EBV-infected Burkitt's lymphoma cell lines Akata, B95-8, Namalwa, and Raji were cultured and transfected as previously described (25, 26, 30, 45–49). NP69 and NP460 are epithelial cell lines immortalized with SV40 T antigen and are commonly regarded as the non-NPC counterpart of C666-1 (25, 30, 31).

Transfection of cells with 100 nM of pre-miR miRNA precursor (Ambion), 150 nM of anti-miR miRNA inhibitor (Ambion), or 100 nM siRNA against PUMA mRNA (siPUMA; Thermo Fisher Scientific) was performed using Lipofectamine 2000 (Invitrogen). Pre-miR miRNA precursors are small chemically modified double-stranded RNA molecules designed to mimic endogenous mature miRNAs. Anti-miR miRNA inhibitors are chemically modified single-stranded nucleic acids designed to specifically bind to and inhibit the activity of endogenous miRNAs. siPUMA is an siRNA that targets nt 715–733 of PUMA mRNA (GenBank NM_014417). Pre-miR, anti-miR, and siPUMA oligonucleotides are ready-to-use reagents with validated activity and specificity.

Dual luciferase reporter assay was performed as previously described (45, 50) using Dual-Luciferase reporter assay system (Promega). The readouts of luciferase activity were taken in an LB 96V microplate luminometer (EG&G Berthold).

Plasmid construction. miR-BART expression vectors (pmiR-BART) were made by inserting miR-BARTs into pSuper vector (provided by R. Agami, Netherlands Cancer Institute, Amsterdam, Netherlands) (22). miR-BARTs were PCR-amplified using genomic DNA of C666-1 cells as template. Primers for amplification of miR-BART5 (nt 946–1196, available at GenBank/EMBL/DDBJ under accession no. EF102892) were 5′-GGAAGATCTATAGAGACACAAGGACTGCCAGCC-3′ (forward) and 5′-CCCAAGCTTCAAAAAACAAGAGCACACACCCACTGTATC-3′ (reverse). Firefly luciferase reporter plasmid pGL3-PUMA.UTR bearing four copies of the miR-BART5 target site found in 3′ UTR of PUMA was constructed by inserting PUMA sequences (nt 1331–1460, available at GenBank/EMBL/DDBJ under accession no. NM_014417) into the XbaI site of pGL3-Control, which is located immediately after the stop codon of the luciferase gene (Promega). As controls, luciferase reporter plasmid pGL3-GAPDH.UTR contains four copies of irrelevant sequences derived from GAPDH, whereas pGL3-BART5.UTR carries four repeats of sequences perfectly complementary to miR-BART5. pGL3-mutPUMA.UTR was derived from pGL3-PUMA.UTR, with the change of 4 nt introduced with QuikChange site-directed mutagenesis kit (Stratagene). As for reporter plasmid pGL3-PUMA.FL.UTR, a single copy of the entire 3′ UTR of PUMA was cloned by PCR amplification of nt 878–1695 in PUMA gene (available at GenBank/EMBL/DDBJ under accession no. NM_014417) and then inserted into the XbaI site of pGL3-Control. In plasmid pGL3-PUMA.FL.rUTR, the reverse sequence of PUMA 3′ UTR was inserted. PUMA cDNA was supplied by B. Vogelstein (Johns Hopkins University, Baltimore, MD) and K. Vousden (the Beatson Institute for Cancer Research, Glasgow, UK).

RNA analysis. 50 μg of total RNA extracted from cultured cells using Trizol reagent (Invitrogen) was subjected to Northern blotting as detailed elsewhere (45). cDNA was also synthesized from Trizol-extracted RNA with ThermoScript reagents (Invitrogen). Semiquantitative PCR was performed with 2 μl of the synthesized cDNA using the following thermal cycling profile: 94°C for 5 min, 30 cycles of amplification (94°C for 1 min, 55°C for 20 s, and 72°C for 45 s), and 72°C for 7 min.

Tumor samples. For Northern blot analysis, NPC tumor biopsies voluntarily donated by 15 individuals were obtained from the Department of Anatomical and Cellular Pathology at the Prince of Wales Hospital (Chinese University of Hong Kong). Human experiments were approved by Joint Clinical Research Ethics Committee of the Chinese University of Hong Kong and Hospital Authority New Territories East Cluster. 75% of the NPC patients were male, whereas two patients were males in the control group. The age of subjects ranged from 25 to 71 yr old. The NPC patients were diagnosed with primary NPC of stages 1–4 (51), except for one patient who had local nasopharyngeal recurrent of NPC. For Western blot analysis, ∼30 pairs of matched NPC and non-NPC samples of the same individual were obtained from Queen Mary Hospital (University of Hong Kong) with the consent of patients for tissue donation. Human experiments were approved by Institutional Review Board of the University of Hong Kong and Hospital Authority Hong Kong West Cluster. 65% of the patients were male. The age of patients ranged from 41 to 68 yr old. Biopsies were taken and endoscopic assessment of the nasopharynx was performed before the start of treatment. Matched samples were taken from the tumor and the grossly unaffected side of nasopharynx for study. All tumor specimens were histologically evaluated to be undifferentiated carcinoma, except for one patient who had poorly differentiated squamous carcinoma. The patients were diagnosed to have primary NPC of stages 1–4 (51). All samples were snap frozen in liquid nitrogen and stored at −80°C until lysed with RIPA for Western blot analysis. Generally consistent with previous findings (27), all NPC samples tested for PUMA expression were positive for EBER and BART transcripts by RT-PCR, whereas all non-NPC tissues were negative for EBER or BART.

Western blotting. RIPA buffer (50 mM Tris-Cl, pH 7.4, 150 mM NaCl, 1% Triton X-100, 0.1% SDS, and 1% sodium deoxycholate) was used to lyse the cells for SDS-PAGE analysis (45, 50). The primary antibodies included a rabbit monoclonal against PUMA (Abcam), a mouse monoclonal against p53 (Santa Cruz Biotechnology, Inc.), a rabbit polyclonal against PARP (Cell Signaling Technology), and a mouse monoclonal antibody against α-tubulin or β-actin (Sigma-Aldrich). The anti-PUMA antibody preferentially reacts with PUMA-β, but the PUMA-α isoform can also be detected in some cells.

Apoptosis assays. PARP cleavage in apoptotic cells was monitored by Western blotting. TUNEL assay was performed by confocal microscopy with fluorescein-based reagents (in situ cell death detection kit; Roche).

Online supplemental material. Fig. S1 shows the expression of miR-BARt5 in EBV-infected cells and tissues. Fig. S2 presents the comparison

of PUMA 3′ UTR activity in HK1 and HK1/EBV cells. Fig. S3 demonstrates the influence of anti–miR-BART5 on PUMA 3′ UTR activity in C666-1 cells. Fig. S4 and Fig. S5 are representative images that demonstrate the induction of apoptosis in C666-1 cells through activation of PUMA expression and inhibition of miR-BART5, respectively. Fig. S6 shows the induction of apoptosis in AGS/BX1 cells through inhibition of miR-BART5. Table S1 lists the potential targets of miR-BART5 predicted by miRanda and RNAhybrid. Online supplemental material is available at http://www.jem.org/cgi/content/full/jem.20072581/DC1.

We thank Reuven Agami, Bert Vogelstein, and Karen Vousden for gifts of plasmid; Honglin Chen and Benjamin Wong for providing AGS and AGS/BX1 cells; Annie Cheung, Wilson Ching, Xin-Yuan Guan, Kwok-Wai Lo, Randy Poon, and Qian Tao for comments and suggestions; and Abel Chun, James Ng, and Vincent Tang for critical reading of the manuscript.

This work was supported by Association for International Cancer Research (07-024) and Fogarty International Center of National Institutes of Health (R01 TW06186-01).

The authors have no conflicting financial interests.

Submitted: 6 December 2007
Accepted: 11 September 2008

REFERENCES

1. Klein, E., L.L. Kis, and G. Klein. 2007. Epstein-Barr virus infection in humans: from harmless to life endangering virus-lymphocyte interactions. *Oncogene*. 26:1297–1305.
2. Tao, Q., L.S. Young, C.B. Woodman, and P.G. Murray. 2006. Epstein-Barr virus (EBV) and its associated human cancers-genetics, epigenetics, pathobiology and novel therapeutics. *Front. Biosci*. 11:2672–2713.
3. Pfeffer, S., M. Zavolan, F.A. Grässer, M. Chien, J.J. Russo, J. Ju, B. John, A.J. Enright, D. Marks, C. Sander, and T. Tuschl. 2004. Identification of virus- encoded microRNAs. *Science*. 304:734–736.
4. Cai, X., A. Schäfer, S. Lu, J.P. Bilello, R.C. Desrosiers, R. Edwards, N. Raab-Traub, and B.R. Cullen. 2006. Epstein-Barr virus microRNAs are evolutionarily conserved and differentially expressed. *PLoS Pathog*. 2:e23.
5. Grundhoff, A., C.S. Sullivan, and D. Ganem. 2006. A combined computational and microarray-based approach identifies novel microRNAs encoded by human gamma-herpesviruses. *RNA*. 12:733–750.
6. Rana, T.M. 2007. Illuminating the silence: understanding the structure and function of small RNAs. *Nat. Rev. Mol. Cell Biol*. 8:23–36.
7. Kim, D.N., H.-S. Chae, S.T. Oh, J.-H. Kang, C.H. Park, W.S. Park, K. Takada, J.M. Lee, W.-K. Lee, and S.K. Lee. 2007. Expression of viral microRNAs in Epstein-Barr virus-associated gastric carcinoma. *J. Virol*. 81:1033–1036.
8. Barth, S., T. Pfuhl, A. Mamiani, C. Ehses, K. Roemer, E. Kremmer, C. Jäker, J. Höck, G. Meister, and F.A. Grässer. 2008. Epstein-Barr virus-encoded microRNA miR-BART2 down-regulates the viral DNA polymerase BALF5. *Nucleic Acids Res*. 36:666–675.
9. Xing, L., and E. Kieff. 2007. Epstein-Barr Virus BHRF1 micro and stable RNAs in Latency III and after induction of replication. *J. Virol*. 81:9967–9975.
10. Xia, T., A. O'Hara, I. Araujo, J. Barreto, E. Carvalho, J.B. Sapucaia, J.C. Ramos, E. Luz, C. Pedroso, M. Manrique, et al. 2008. EBV microRNAs in primary lymphomas and targeting of CXCL-11 by ebv-mir-BHRF1-3. *Cancer Res*. 68:1436–1442.
11. Lo, A.K.F., K.F. To, K.W. Lo, R.W.M. Lung, J.W.Y. Hui, G. Liao, and S.D. Hayward. 2007. Modulation of LMP1 protein expression by EBV-encoded microRNAs. *Proc. Natl. Acad. Sci. USA*. 104:16164–16169.
12. Han, J., C. Flemington, A.B. Houghton, Z. Gu, G.P. Zambetti, R.J. Lutz, L. Zhu, and T. Chittenden. 2001. Expression of bbc3, a pro-apoptotic BH3-only gene, is regulated by diverse cell death and survival signals. *Proc. Natl. Acad. Sci. USA*. 98:11318–11323.
13. Nakano, K., and K.H. Vousden. 2001. PUMA, a novel proapoptotic gene, is induced by p53. *Mol. Cell*. 7:683–694.
14. Yu, J., L. Zhang, P.M. Hwang, K.W. Kinzler, and B. Vogelstein. 2001. PUMA induces the rapid apoptosis of colorectal cancer cells. *Mol. Cell*. 7:673–682.
15. Wang, P., J. Yu, and L. Zhang. 2007. The nuclear function of p53 is required for PUMA-mediated apoptosis induced by DNA damage. *Proc. Natl. Acad. Sci. USA*. 104:4054–4059.
16. Jeffers, J.R., E. Parganas, Y. Lee, C. Yang, J. Wang, J. Brennan, K.H. MacLean, J. Han, T. Chittenden, J.N. Ihle, et al. 2003. Puma is an essential mediator of p53-dependent and -independent apoptotic pathways. *Cancer Cell*. 4:321–328.
17. Concannon, C.G., B.F. Koehler, C. Reimertz, B.M. Murphy, C. Bonner, N. Thurow, M.W. Ward, A. Villunger, A. Strasser, D. Kögel, and J.H. Prehn. 2007. Apoptosis induced by proteasome inhibition in cancer cells: predominant role of the p53/PUMA pathway. *Oncogene*. 26:1681–1692.
18. Enright, A.J., B. John, U. Gaul, T. Tuschl, C. Sander, and D.S. Marks. 2003. MicroRNA targets in *Drosophila*. *Genome Biol*. 5:R1.
19. John, B., A.J. Enright, A. Aravin, T. Tuschl, C. Sander, and D.S. Marks. 2004. Human MicroRNA targets. *PLoS Biol*. 2:e363.
20. Rehmsmeier, M., P. Steffen, M. Hochsmann, and R. Giegerich. 2004. Fast and effective prediction of microRNA/target duplexes. *RNA*. 10:1507–1517.
21. Sethupathy, P., M. Megraw, and A.G. Hatzigeorgiou. 2006. A guide through present computational approaches for the identification of mammalian microRNA targets. *Nat. Methods*. 3:881–886.
22. Brummelkamp, T.R., R. Bernards, and R. Agami. 2002. A system for stable expression of short interfering RNAs in mammalian cells. *Science*. 296:550–553.
23. Cheung, S.T., D.P. Huang, A.B. Hui, K.W. Lo, C.W. Ko, Y.S. Tsang, N. Wong, B.M. Whitney, and J.C. Lee. 1999. Nasopharyngeal carcinoma cell line (C666-1) consistently harbouring Epstein-Barr virus. *Int. J. Cancer*. 83:121–126.
24. Huang, D.P., J.H. Ho, Y.F. Poon, E.C. Chew, D. Saw, M. Lui, C.L. Li, L.S. Mak, S.H. Lai, and W.H. Lau. 1980. Establishment of a cell line (NPC/HK1) from a differentiated squamous carcinoma of the nasopharynx. *Int. J. Cancer*. 26:127–132.
25. Lo, A.K.F., K.W. Lo, S.W. Tsao, H.L. Wong, J.W. Hui, K.F. To, D.S. Hayward, Y.L. Chui, Y.L. Lau, K. Takada, and D.P. Huang. 2006. Epstein-Barr virus infection alters cellular signal cascades in human nasopharyngeal epithelial cells. *Neoplasia*. 8:173–180.
26. Borza, C.M., and L.M. Hutt-Fletcher. 2002. Alternate replication in B cells and epithelial cells switches tropism of Epstein-Barr virus. *Nat. Med*. 8:594–599.
27. Zhou, L., W. Jiang, C. Ren, Z. Yin, X. Feng, W. Liu, Q. Tao, and K. Yao. 2005. Frequent hypermethylation of RASSF1A and TSLC1, and high viral load of Epstein-Barr Virus DNA in nasopharyngeal carcinoma and matched tumor- adjacent tissues. *Neoplasia*. 7:809–815.
28. Liu, J., M.A. Valencia-Sanchez, G.J. Hannon, and R. Parker. 2005. MicroRNA- dependent localization of targeted mRNAs to mammalian P-bodies. *Nat. Cell Biol*. 7:719–723.
29. Mathonnet, G., M.R. Fabian, Y.V. Svitkin, A. Parsyan, L. Huck, T. Murata, S. Biffo, W.C. Merrick, E. Darzynkiewicz, R.S. Pillai, et al. 2007. MicroRNA inhibition of translation initiation in vitro by targeting the cap-binding complex eIF4F. *Science*. 317:1764–1767.
30. Tsao, S.W., X. Wang, Y. Liu, Y.C. Cheung, H. Feng, Z. Zheng, N. Wong, P.W. Yuen, A.K.P. Lo, Y.C. Wong, and D.P. Huang. 2002. Establishment of two immortalized nasopharyngeal epithelial cell lines using SV40 large T and HPV16 E6/E7 viral oncogenes. *Biochim. Biophys. Acta*. 1590:150–158.
31. Wong, H.L., X. Wang, R.C.-C. Cheng, D.-Y. Jin, H. Feng, Q. Wang, K.W. Lo, D.P. Huang, P.W. Yuen, K. Takada, et al. 2005. Stable expression of EBERs in immortalized nasopharyngeal epithelial cells confers resistance to apoptotic stress. *Mol. Carcinog*. 44:92–101.
32. Oliver, F.J., G. de la Rubia, V. Rolli, M.C. Ruiz-Ruiz, G. de Murcia, and J.M. Murcia. 1998. Importance of poly(ADP-ribose) polymerase and its cleavage in apoptosis. Lesson from an uncleavable mutant. *J. Biol. Chem*. 273:33533–33539.
33. Dykxhoorn, D.M. 2007. MicroRNAs in viral replication and pathogenesis. *DNA Cell Biol*. 26:239–249.
34. Stern-Ginossar, N., N. Elefant, A. Zimmermann, D.G. Wolf, N. Saleh, M. Biton, E. Horwitz, Z. Prokocimer, M. Prichard, G. Hahn, et al. 2007. Host immune system gene targeting by a viral miRNA. *Science*. 317:376–381.

35. Murphy, E., J. Vaničček, H. Robins, T. Shenk, and A.J. Levine. 2008. Suppression of immediate-early viral gene expression by herpesvirus-coded microRNAs: implications for latency. *Proc. Natl. Acad. Sci. USA*. 105:5453–5458.
36. Li, L.Y., M.Y. Liu, H.M. Shih, C.H. Tsai, and J.Y. Chen. 2006. Human cellular protein VRK2 interacts specifically with Epstein-Barr virus BHRF1, a homologue of Bcl-2, and enhances cell survival. *J. Gen. Virol.* 87:2869–2878.
37. Smith, P.R., O. de Jesus, D. Turner, M. Hollyoake, C.E. Karstegl, B.E. Griffin, L. Karran, Y. Wang, S.D. Hayward, and P.J. Farrell. 2000. Structure and coding content of CST (BART) family RNAs of Epstein-Barr virus. *J. Virol.* 74:3082–3092.
38. Zhang, J., H. Chen, G. Weinmaster, and S.D. Hayward. 2001. Epstein-Barr virus BamHI-A rightward transcript-encoded RPMS protein interacts with the CBF1-associated corepressor CIR to negatively regulate the activity of EBNA2 and NotchIC. *J. Virol.* 75:2946–2956.
39. He, L., X. He, S.W. Lowe, and G.J. Hannon. 2007. microRNA join the p53 network – another piece in the tumour-suppression puzzle. *Nat. Rev. Cancer.* 7:819–822.
40. Skalsky, R.L., M.A. Samols, K.B. Plaisance, I.W. Boss, A. Riva, M.C. Lopez, H.V. Baker, and R. Renne. 2007. Kaposi's sarcoma-associated herpesvirus encodes an ortholog of miR-155. *J. Virol.* 81:12836–12845.
41. Gottwein, E., N. Mukherjee, C. Sachse, C. Frenzel, W.H. Majoros, J.T. Chi, R. Braich, M. Manoharan, J. Soutschek, U. Ohler, and B.R. Cullen. 2007. A viral microRNA functions as an orthologue of cellular miR-155. *Nature*. 450:1096–1099.
42. Gottwein, E., and B.R. Cullen. 2008. Viral and cellular microRNAs as determinants of viral pathogenesis and immunity. *Cell Host Microbe*. 3:375–387.
43. Effert, P., R. McCoy, M. Abdel-Hamid, K. Flynn, Q. Zhang, P. Busson, T. Tursz, E. Liu, and N. Raab-Traub. 1992. Alterations of the p53 gene in nasopharyngeal carcinoma. *J. Virol.* 66:3768–3775.
44. Li, L., L. Guo, Y. Tao, S. Zhou, Z. Wang, W. Luo, D. Hu, Z. Li, L. Xiao, M. Tang, et al. 2007. Latent membrane protein 1 of Epstein-Barr virus regulates p53 phosphorylation through MAP kinases. *Cancer Lett.* 255:219–231.
45. Choy, E.Y.W., K.H. Kok, S.W. Tsao, and D.Y. Jin. 2008. Utility of Epstein-Barr virus-encoded small RNA promoters for driving the expression of fusion transcripts harboring small hairpin RNAs. *Gene Ther.* 15:191–202.
46. Cheung, H.W., Y.P. Ching, J.M. Nicholls, M.T. Ling, Y.C. Wong, N. Hui, A. Cheung, S.W. Tsao, Q. Wang, P.W. Yeun, et al. 2005. Epigenetic inactivation of CHFR in nasopharyngeal carcinoma through promoter methylation. *Mol. Carcinog.* 43:237–245.
47. Cheung, H.W., D.Y. Jin, M.T. Ling, Y.C. Wong, Q. Wang, S.W. Tsao, and X. Wang. 2005. Mitotic arrest deficient 2 expression induces chemosensitization to a DNA-damaging agent, cisplatin, in nasopharyngeal carcinoma cells. *Cancer Res.* 65:1450–1458.
48. Chen, H., J. Huang, F.Y. Wu, G. Liao, L. Hutt-Fletcher, and S.D. Hayward. 2005. Regulation of expression of the Epstein-Barr virus BamHI-A rightward transcripts. *J. Virol.* 79:1724–1733.
49. Chan, S.Y.Y., K.W. Choy, S.W. Tsao, T. Qian, T. Tang, G.T.Y. Chung, and K.W. Lo. 2008. Authentication of nasopharyngeal carcinoma tumor lines. *Int. J. Cancer.* 122:2169–2171.
50. Kok, K.H., M.H.J. Ng, Y.P. Ching, and D.Y. Jin. 2007. Human TRBP and PACT interact with each other and associate with Dicer to facilitate the production of small interfering RNA. *J. Biol. Chem.* 282:17649–17657.
51. American Joint Committee on Cancer. 2002. AJCC Cancer Staging Manual. 6th edition, Springer-Verlag Publishers, New York, pp. 50-52.